PNAS

Supporting Information for

Mechanism of 30S subunit recognition and modification by the conserved bacterial ribosomal RNA methyltransferase RsmI

Mohamed I. Barmada[1,2], Erin N. McGinity[1], Suparno Nandi[1], Debayan Dey[1], Natalia Zelinskaya[1], George M. Harris[3], Lindsay R. Comstock[3], Christine M. Dunham[4] and Graeme L. Conn[1]*

[1]Department of Biochemistry, Emory University School of Medicine, Atlanta, Georgia, 30322, USA

[2]Graduate Program in Biochemistry, Cell and Developmental Biology, Emory University, Atlanta, Georgia, 30322, USA

[3]Department of Chemistry, Wake Forest University, Winston-Salem, North Carolina, 27106, USA

[4]Department of Chemistry, Emory University, Atlanta, Georgia, 30322, USA

Corresponding author: Graeme L. Conn
Email: gconn@emory.edu

This PDF file includes:

Figures S1 to S8
Tables S1 to S3
SI Methods
RsmI protein expression, purification and site-directed mutagenesis
Cryo-EM image processing
[^{3}H]-SAM methyltransferase assays to assess impact of 30S subunit activation and divalent metal ion identity on RsmI activity
RsmI conservation analysis
Isothermal titration calorimetry

Supplementary Figures

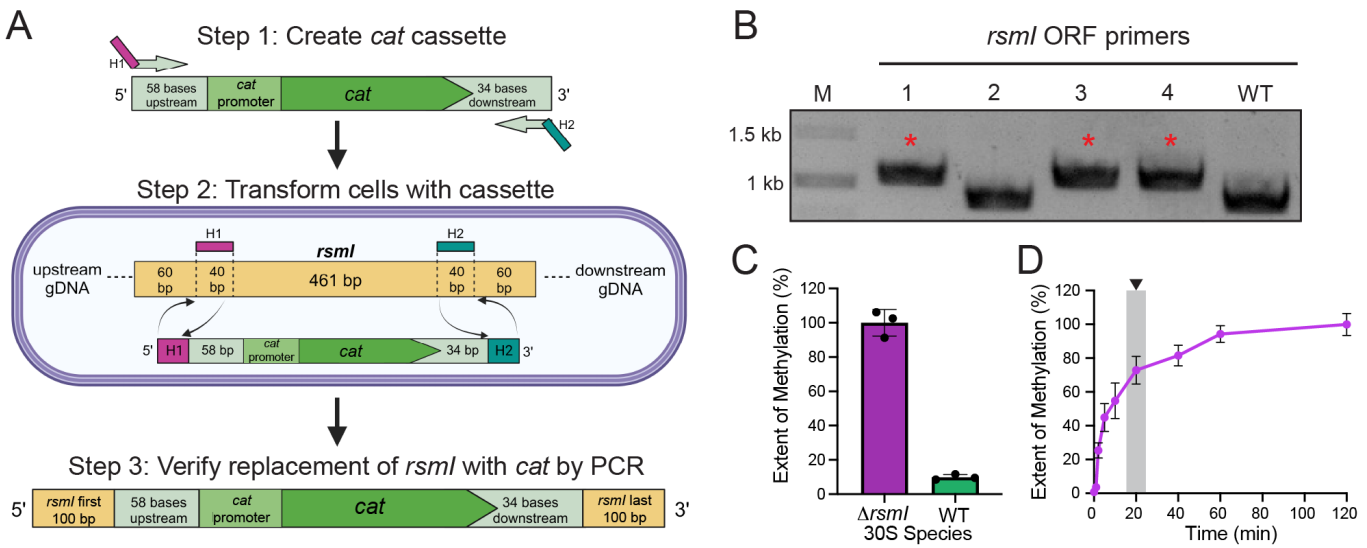

Fig. S1. Sample preparation for structure-function analyses of the RsmI-30S complex. (*A*) Scheme depicting *rsmI* deletion by replacement with a DNA cassette encoding the chloramphenicol acetyltransferase gene (*cat*) and its promoter. H1 = 5' homology region, H2 = 3' homology region. (*B*) Verification of *cat* replacement of *rsmI* via PCR. Colonies (1-4) were screened by PCR amplification of genomic DNA using primers targeting the intact 5' and 3' ends of the *rsmI* open reading frame ("*rsmI* ORF primers"). A higher molecular weight band confirms insertion of *cat* (red asterisk). WT = wild-type, M = marker. (*C*) Single time point *in vitro* methylation assay reveals that the activity of RsmI with 30S-Δ*rsmI* is significantly greater than with wildtype (WT) 30S (where this site is already modified by endogenous RsmI), indicating that 30S-Δ*rsmI* is a suitable substrate for structural studies. (*D*) Time-course methylation assay for RsmI and Δ*rsmI* 30S at a 1:1 enzyme to 30S ratio shows that RsmI begins to plateau in its activity at around 20 minutes (indicated by shaded region and arrowhead).

[Image is shown on the following page]

Fig. S2. Cryo-EM processing workflow. (*A*) Preliminary steps including micrograph movie import to CryoSparc, pre-processing in the form of motion correction and CTF estimation, and particle blob picking. (*B*) Particle Curation in the form of particle picking, 2D classification, and 3D sorting through ab-initio reconstruction and heterogenous refinement. (*C*) Iterative refinements jobs in the form of homogenous refinement, local and global CTF refinement, and reference-based motion correction to improve map resolution. (*D*) Additional particle curation in the form of masked 3D classification and heterogenous refinement followed by homogenous refinement to achieve a consensus volume. From this volume, two paths were chosen: (*E*) particle density around RsmI and its tertiary binding surface was subtracted to allow masked local refinement of the enzyme and its 16S rRNA interface to produce a 2.55 Å focused map, and (*F*) further 3D classification with variable filter resolutions was undertaken to remove 30S head-induced heterogeneity and further improve enzyme occupancy to produce, after additional refinement, a 2.42 Å map of the whole complex.

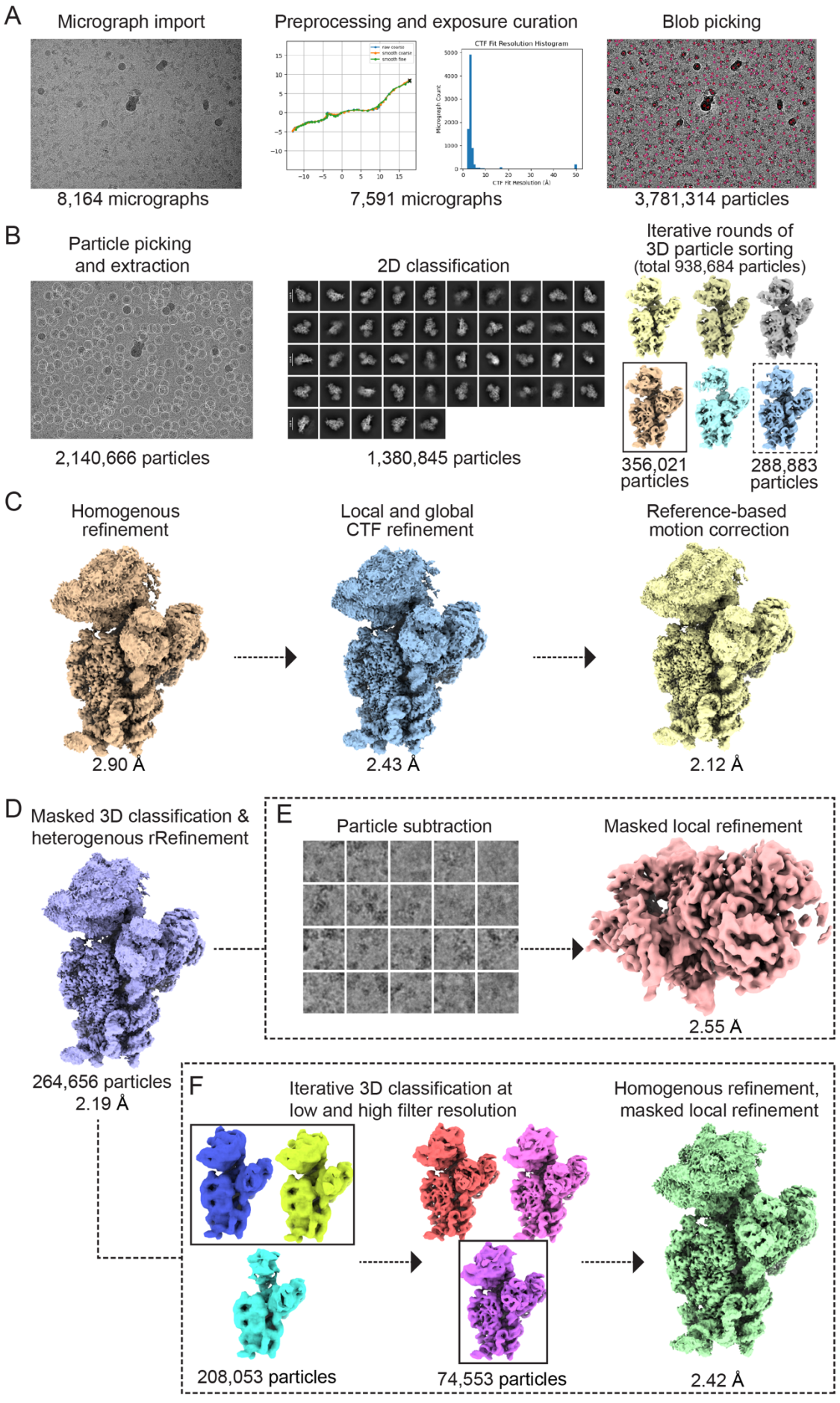

Fig. S2. Cryo-EM processing workflow. *[Full legend is provided on the previous page]*

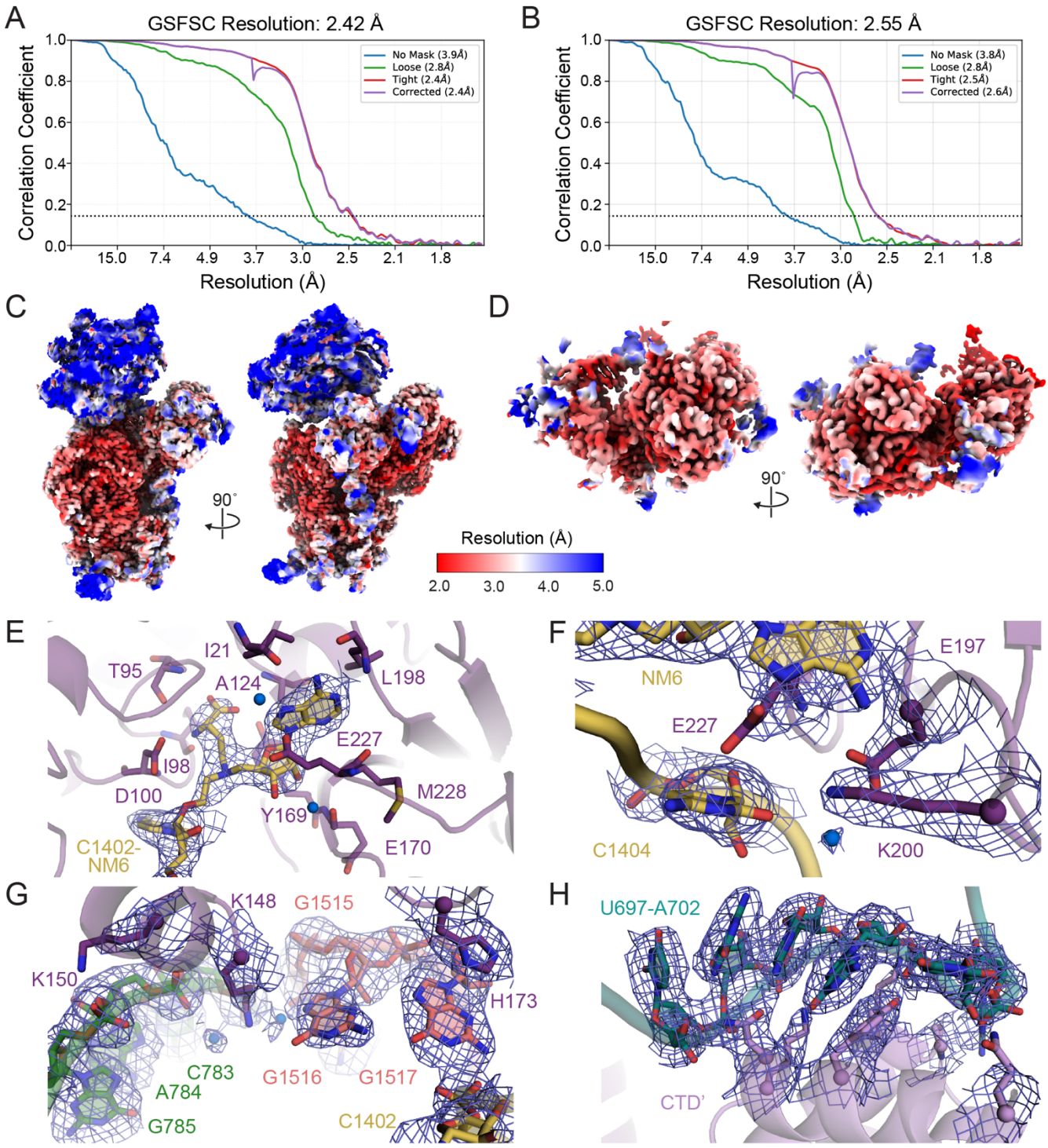

Fig. S3. Map quality analyses. GSFSC curves of the (*A*) 2.42 Å map of the entire RsmI-30S complex and (*B*) 2.55 Å map of RsmI and its 16S rRNA binding surface. Local resolution estimates shown as representative views for (*C*) the full RsmI-30S subunit complex and (*D*) RsmI and its 16S rRNA binding surface. Representative views of map quality for the 2.55 Å focused map highlighting (*E*) the target nucleotide C1402 covalently attached to the SAM analog NM6 (contour level 17σ) and RsmI residues in contact with (*F*) h44 nucleotide C1404 (contour level 15σ for protein/ RNA and 9σ for water), (*G*) h24a and h45 (contour level 15σ for protein/ RNA and 7σ for water), and (*H*) h23b (contour level 15σ for RNA and 10σ for RsmI).

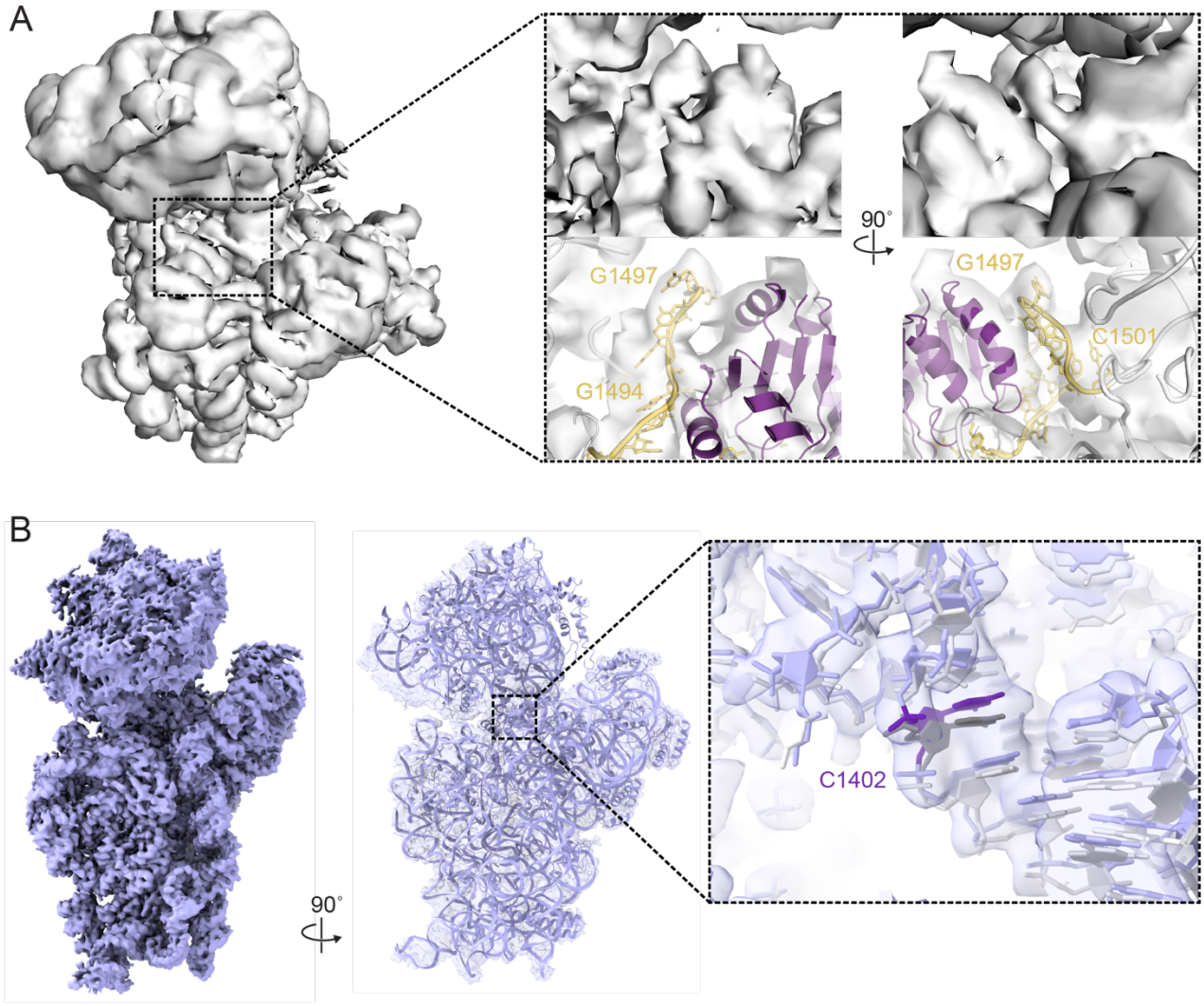

Fig. S4. Additional maps generated during cryo-EM processing. (*A*) Low-resolution map (6 Å) of the entire RsmI-30S complex with zoomed-in views of the map (*top*) corresponding to the dynamic h44 region (residues 1494-1501) and the final model in the semi-transparent map (*bottom*). (*B*) 2.91 Å map of the free 30S-Δ*rsmI* (*left*) with the free 30S-Δ*rsmI* structure (**Table S1**, PDB 10FZ) overlaid (*right*). The zoomed-in view shows the h44 region around C1402 (violet) from the free 30S-Δ*rsmI* structure superimposed on a wild-type 30S model (PDB 7OE1; C1402 in dark grey), with both models overlaid on the free 30S-Δ*rsmI* map (ChimeraX threshold = 0.119). The two models align well (RSMD = 0.90) and occupy the same density in the map, indicating that the free 30S-Δ*rsmI* and wild-type 30S are essentially identical in structure.

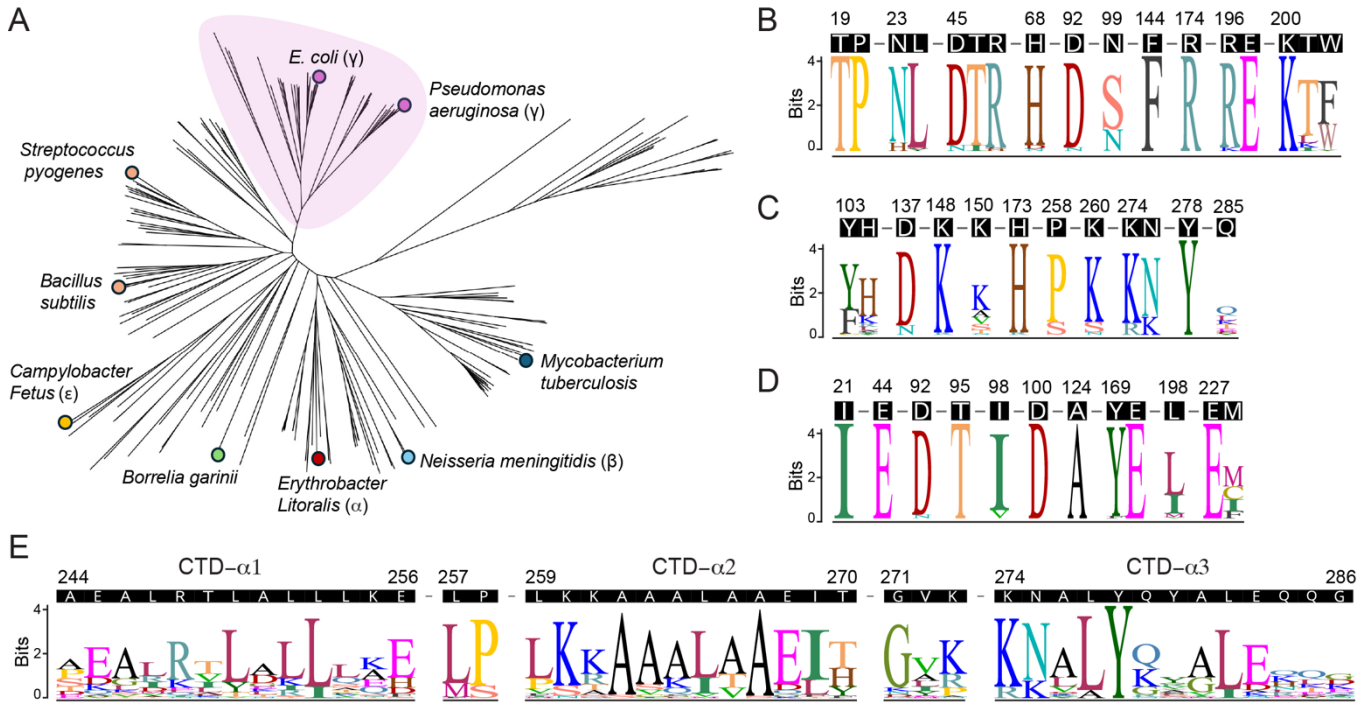

Fig. S5. Conservation of RsmI among bacterial species and key functional residues among RsmI orthologs. (*A*) Neighbor-joining phylogenetic tree displaying the distribution of RsmI among key bacterial families, with the Gammaproteobacterial RsmI clade highlighted (purple shading). Sequence logo of Gammaproteobacterial RsmI sequences showing propensities for (*B*) residues involved h44 interaction, (*C*) 30S platform contact, and (*D*) SAM binding and Mg^{2+} ion coordination. **E.** Sequence logo of Gammaproteobacterial RsmI sequences showing the residue conservation for the CTD domain. All sequence logo plots are accompanied by the *E. coli* RsmI sequence above them as reference.

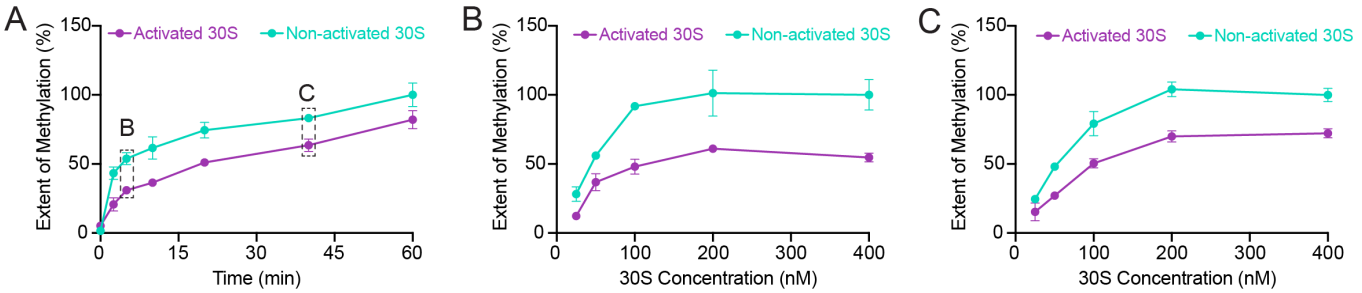

Fig. S6. 30S subunit activation influences RsmI methylation activity *in vitro*. (*A*) Time-course methylation assay for RsmI and Δ*rsmI* 30S under activating and non-activating conditions at a 1:1 enzyme to 30S ratio. Using the time-course as a guide, the impact of activation was compared by altering 30S subunit concentration at two time points: (*B*) early in the time course (5 minutes) and (*C*) near the reaction plateau (40 minutes) while keeping the enzyme concentration constant.

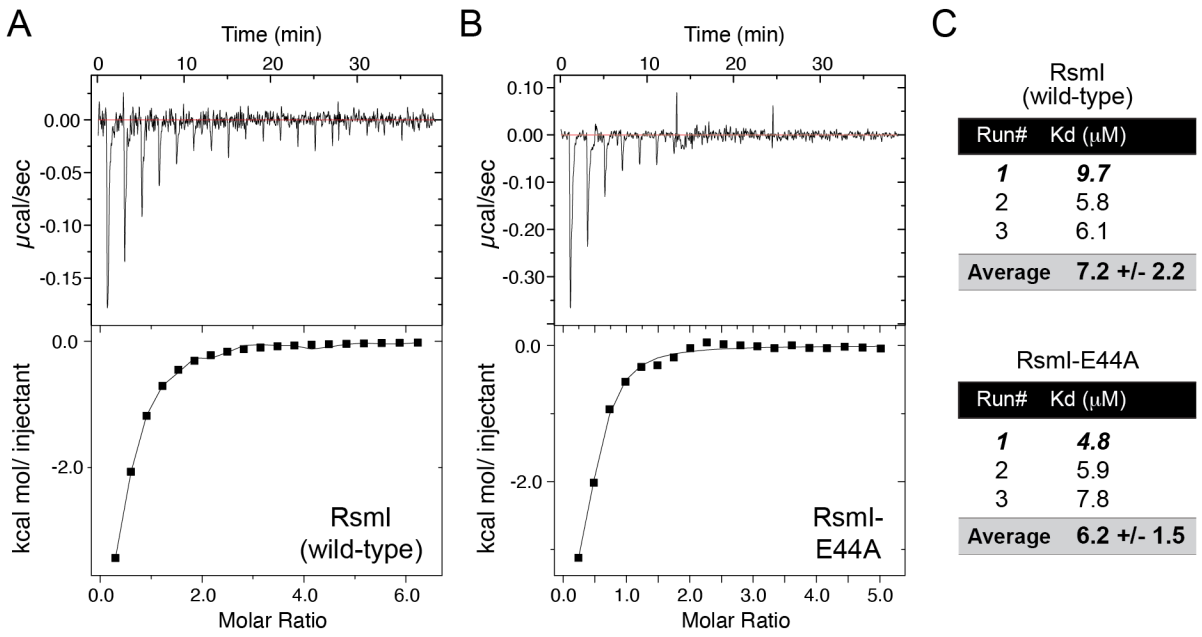

Fig. S7. The E44A substitution does not impact SAM binding. Representative ITC experiments (*top*, raw titration thermogram and *bottom*, integrated heats) for titration of SAM into (*A*) wild-type RsmI and (*B*) the RsmI E44A variant. (*C*) Individual and average K_d values obtained from the triplicate ITC experiments with each protein.

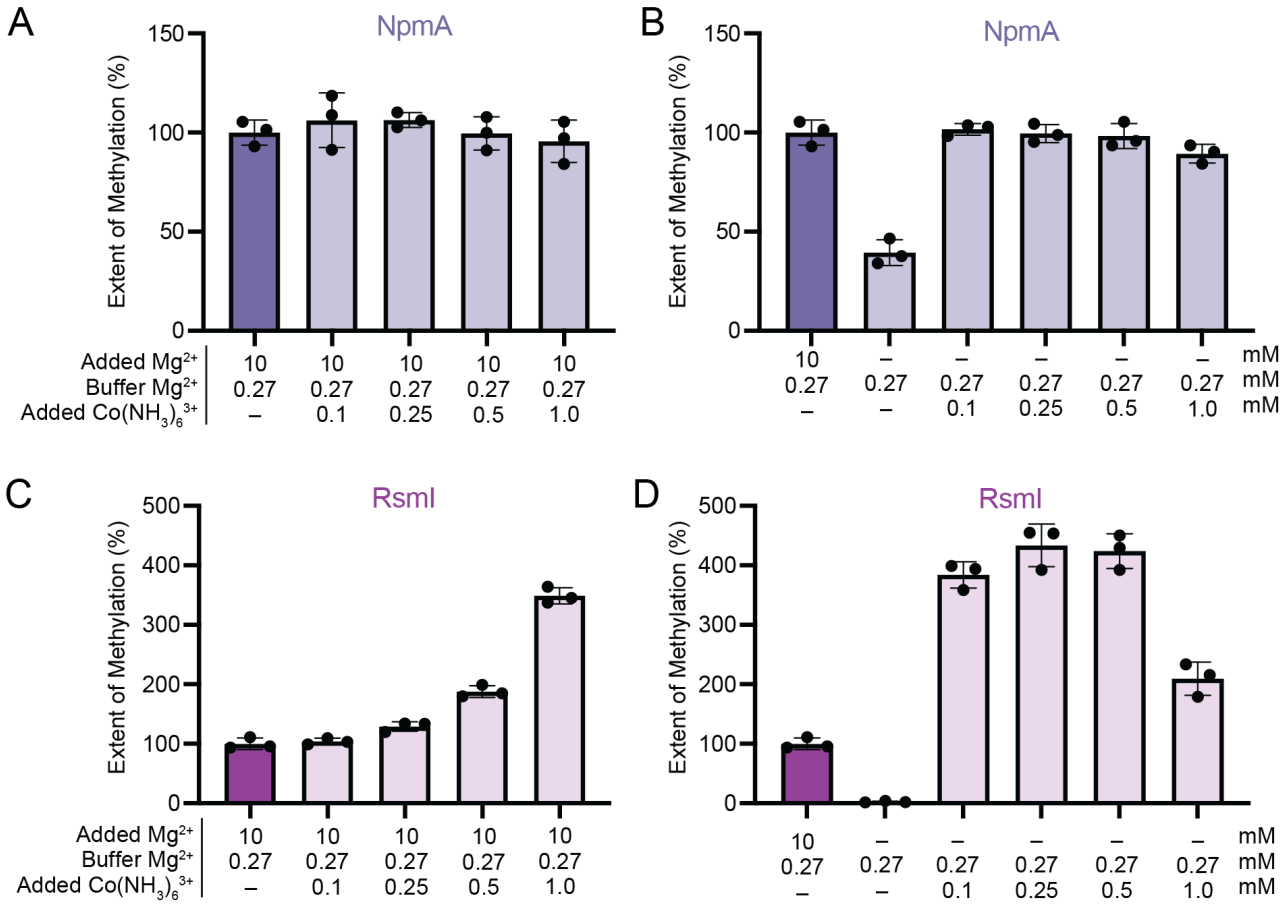

Fig. S8: Methyltransferase assays with $Co(NH_3)_6^{3+}$ suggest that the divalent ion in the RsmI active site plays a predominantly structural role in coordinating C1402 for 2'-O-modification. *In vitro* methyltransferase activity assays with $Co(NH_3)_6^{3+}$ titrated from 0 to 1 mM for NpmA with (*A*) 10 mM Mg^{2+} or (*B*) no additional Mg^{2+} in the reaction buffer. (*C,D*) As for *panels A* and *B* but for RsmI.

Supplementary Tables

Table S1. Cryo-EM data collection, refinement, and model validation statistics

	RsmI-30S subunit (full complex)	RsmI-16S rRNA (binding interface)[a,b]	30S-Δ*rsmI* (no RsmI)[b]
Deposition			
Coordinates (PDB)	9PZG		10FZ
Map (EMDB)	EMD-72071		EMD-75144
Data Collection			
Magnification	×105,000		
Voltage (kV)	300		
Electron exposure (e^-/Å^2)	49.27		
Defocus range (μm)	-0.4 to -2.9		
Pixel size (Å)	0.41		
Symmetry imposed	C1		
Initial particle count	3,781,314		
Final particle count	74,553	264,656	58,273
Map resolution (Å)			
($FSC_{0.143}$, masked)	2.42	2.55	2.91
Refinement			
Model resolution (Å)			
($FSC_{0.143/0.5}$, masked)	2.43/2.92	2.57/2.92	2.91/3.21
d_model	2.70	2.90	3.00
CC_{mask}	0.84	0.87	0.79
Model composition			
Nonhydrogen atoms	55,584	6,345	51,092
Protein residues	2,868	549	2,320
Nucleotides	1,529	95	1,530
Ligands			
NM6 (AN6)	2	2	–
Mg^{2+}	79	1	77
Water	170	18	32
ADP (B-factors)			
Protein (min/max/mean)	23.8/ 636.0/ 179.8	24.6/636.0/141.7	46.8/664.2/243.3
Nucleotide (min/max/mean)	20.0/430.4/159.4	20.0/220.1/92.8	40.7/980.9/244.6
Ligand (min/max/mean)	30.0/135.7/67.8	68.2/68.2/68.2	47.6/121.9/72.5
Water (min/max/mean)	10.0/515.0/85.9	10.0/515.0/119.6	66.8/1132.3/280.8
R.M.S. deviations			
Bond lengths (Å)	0.004	0.010	0.002
Bond angles (°)	0.764	1.287	0.459
Validation			
MolProbity score	1.89	1.48	1.89
Clashscore	6.84	6.82	7.89
Rotamer outliers (%)	1.66	1.38	0.05
Ramachandran plot			
Favored (%)	95.0	98.3	92.6
Allowed (%)	5.0	1.7	7.3
Outliers (%)	0.0	0.0	0.0

[a]Processing and refinement statistics for the focused map of the RsmI-30S subunit interface and corresponding truncated model comprising RsmI and its 16S rRNA tertiary surface (see Materials and Methods for further details).
[b]Data collection parameters are identical to those for the RsmI-30S subunit (full complex) as the three structures were determined using the same image data set.

Table S2. Conservation of select residues among RsmI family methyltransferases

Residue	Interaction	Residue identity (% occurrence)[a,b]	
		All	γ-Proteobacteria
T19	A1408	T (91.9)	T (100)
P20	A1408	P (92.4)	P (100)
I21	SAM	I (82.3), L(11.6)	I (100)
N23	C1407	N (79.8), D (8.6), E (5.6)	N (90.7), H (9.3)
L24	A1408	L (69.2), V (6.1), I (4.0)	L (95.3), Y (2.3), M (2.3)
E44	Mg^{2+}	E (100)	E (100)
D45	C1400	D (90.4), N (7.1)	D (93), N (7)
T46	C1400	T (87.9), A (3.5), E (3)	T (93), I (7)
R47	C1400	R (91.4), K (7.1)	R (95.3), H (2.3), F (2.3)
H68	G1401	H (71.7), G (7.6), F (6.1),	H (93)
D92	A1408	D (90.9), E (8.1)	D (95.3), N (4.7)
T95	SAM	T (48.0), M (35.4), L (7.1)	T (100)
I98	SAM	I (67.7), V (30.3)	I (90.7), V (9.3)
N99	C1402	S (81.3), A (8.6), N (8.1)	S (72.1), N (27.9)
D100	SAM/ Mg^{2+}	D (100)	D (100)
Y103	A790	Y (41.4), F (17.7), A (15.7)	Y (62.8), F (34.9)
H104	A790	R (21.7), H (15.2), E (12.1),	H (67.4), K (11.6), R (7)
A124	SAM	A (89.4), S (10.6)	A (100)
D137	A790	D (45.4), N (21.9), E (7.7)	D (88.4), N (11.6)
F144	C1403	F (91.9), Y (8.1)	F (100)
K148	h24-h45	K (78.3), D (6.1), E (4.5)	K (97.7), R (2.3)
K150	h24-h45	K (35), G (29.9), A (9.1)	K (51.2), A (14), V (14)
Y169	SAM	Y (63.6), F (26.8), I (6.6)	Y (97.7), F (2.4)
E170	SAM	E (96)	E (100)
H173	h24-h45	H (65.2), Y (17.7), R (5.6)	H (97.7), R (2.4)
R174	C1403	R (94.4), K (5.6)	R (100)
R196	G1405	R (86.9), K (5.6), A (4)	R (95.3), K (4.7)
E197	C1404	E (90.9), D (4.5), N (3.5)	E (100)
L198	SAM	L (75.8), I (18.7)	L (100)
K200	C1404	K (100), L (4.5)	K (100)
T201	C1407	T (32.8), L (25.3), K (11.1)	T (79.1), L (9.3), K (7.0)
W202	G1405	F (33.3), H (25.3), Y (25.3), W (8.1)	F (60.5), W (37.2)
E227	SAM	E (90.9), P (8.1)	E (100)
M228	SAM	I (34.3), F (26.8), C (14.6)	M (39.5), I (23.3), C (23.3)
R248	CTD (dimer)	R (30.7), A (11.7), L (11)	R (67.4), K (14)
L252	CTD (dimer)	L (35.4), R (14.9), E (7.5)	L (65.1), K (11.6), R (9.3)
L253	CTD (dimer)	L(41.5), I (21.4), V (15.1)	L(86), I (14)
L257	CTD (dimer)	L (40.3), M (16.4), E (11.9)	L (79.1), M (18.6)
P258	h23	P (37.1), R (20.1), S (19.5)	P (83.7), S (16.3)
K260	h23	K (69.4), S (11.5), N (11.5)	K (83.7), S (14)
L265	CTD (dimer)	L (28.8), E (14.1), Q (12.3)	L (69.8), I (23.3)
E268	CTD (dimer)	K (32.7), E (24.7), A (16.7)	E (79.1), D (9.3)
I269	CTD (dimer)	I (26.7), L (13.7), E (12.4)	I (72.1), L (23.3)
K274	h23	K (60.5), R (29.3)	K (86), R (14)
N275	h23	R (32.5), N (28.8), K (18.8)	N (76.7), K (23.3)
Y278	h23	Y (91.8), F (8.2)	Y (100)
Q285	h23	K (37.6), R (14.4), Q (13.6)	Q (33.3), L (16.7), K (13.9), T (13.9)

[a]Residue percentages were calculated for the top three amino acids at each position, unless the third and fourth residues had identical frequencies, in which case all were included

[b]Analysis was performed using all 198 RsmI sequences and a subset of 43 sequences from Gammaproteobacteria.

Table S3. List of primers used in this study

Primer	Sequence 5' to 3'	Purpose
cat-RsmI-Forward	**ATCGGCAATCTGGCGGATATCACCCAGCGTGCGTTAGAGG**CTGGTGTCCCTGTTGATACC	**Figure S1A, Step 1**: Generate *cat* cassette: 40 bp of *rsmI* sequence (bold/ underline) and pZS21 before and after *cat*.
cat-RsmI-Reverse	**TGCGGCCAGCGCCGCCGCTTTTTTCAGCGGCAGTTCTGCC**GCGTTTAAGGGCACCAATAAC	
RsmI-ORF-Forward	GAAGATCTCAT**ATG**AAACAACACCAATCGGC	**Figure S1A, Step 3**: clone *rsmI* into pET-44 and verify *rsmI* deletion. Start/ end of *rsmI* ORF (bold/underline).
RsmI-ORF-Reverse	CTAAAGCTTTTA**TTA**CCCCTGCTGCTCC	
pET-44-RsmI-Forward	GCAACCGCGAATTCACCTGTGG	***rsmI* mutagenesis**: Reverse primer for first-round PCR in MEGAWHOP contains the altered codon (bold/ underlined)
T19Y	CAGATTGCCGATTGG**ATA**CGGTACAATG	
N23Y	GATATCCGCCAG**ATA**GCCGATTGG	
E44A	CGAGTATC**TGC**GGCGGCAATC	
T46A/R47A	GGTGTG**AGCAGC**ATCCTCGG	
R47A	CCGGTGTG**AGC**AGTATCCTC	
H68A	GTTGTTCGTT**AGC**GTCGTGCAG	
D92A	GTTCCGGC**AGC**GGAAACCAG	
Y103A	CACCAGATG**AGC**GCCAGGATC	
Y103A/H104A	GTACGCACCAG**AGCAGC**GCCAGGATCGTTAATTAG	
D137R	GTAACAGAAACG**CCG**AGAGGGTAAAC	
F144A	GCAGGTAA**AGC**GCCTTCGTAAC	
K148E	GGCCTTTTGA**TTC**GGCAGGTAAAAAG	
K148E/K150E	GCC**TTC**TGA**TTC**GGCAGGTAAAAAG	
K150E	GGCGGCC**TTC**TGATTTGG	
H173A	GCTATCTAACAGACG**AGC**GGTAGATTC	
R174A	GCTATCTAACAG**AGC**GTGGGTAGATTC	
R174E	GCTATCTAACAG**CTC**GTGGGTAGATTC	
R196A	GTCAGCTC**AGC**CGCCAGAAC	
R196E	GTCAGCTC**TTC**CGCCAGAAC	
K200A	GTTTCCCAGGT**AGC**GGTCAGCTC	
K200E	GTTTCCAGGTTTCGGTCAGCTC	
W202A	GTGAATGGTTTC**AGC**GGTTTTGGTC	
E227A	CAATCAGCACCAT**AGC**GCCTTTGC	
R248E	GCCAGCGT**TTC**CAGGGCATC	
L253E	GTTCTGCCTG**TTC**CAGCGCCAG	
P258G	GCTTTTTTCAG**ACC**CAGTTCTGC	
K260E	CCGCTTT**TTC**CAGCGGC	
Y278A	CGCATACTT**AGC**CAGCGCATTTTTC	
ΔCTD-α_3	GCATTTTTCTTCAC**TCA**GTGAATTTCTGCG	
ΔCTD	GTCTTCTTCCTG**TCA**TTTATGACCTTCG	

SI Methods

RsmI protein expression, purification and site-directed mutagenesis–The sequence encoding RsmI was PCR amplified from *E. coli* BW25113 genomic DNA (*SI Appendix*, **Table S3**) and subcloned into a pET44a vector with an N-terminal hexahistidine tag (pET44-RsmI). This plasmid was used to transform *E. coli* BL21(DE3) cells with subsequent growth at 37 ˚C in lysogeny broth containing ampicillin (100 µg/ml). Protein expression was induced at mid-log phase (~0.6 OD_{260}) with 1 mM isopropyl β-D-1-thiogalactopyranoside and growth continued for another 3 hours before being harvested via centrifugation at 4˚C. Cells were resuspended in lysis buffer (50 mM HEPES-NaOH, pH 7.6, 1 M NaCl, 10 mM imidazole, 0.5% Triton X-100, and 2 mM β-mercaptoethanol containing the protease inhibitors PMSF and benzamidine) and lysed by sonication (Misonix Sonicator 3000 with microtip: 7.5-min total sonication time, 1-s on, 1-s off, output level 5.0). Cell lysates were cleared by centrifugation at 4˚C and then dialyzed three times (2 x 3 hours and overnight) against a high salt buffer (50 mM HEPES-NaOH, pH 7.6, 2 M NaCl, 10 mM imidazole, and 2 mM mM β-mercaptoethanol) to remove any SAM copurifying with RsmI. The lysate was then dialyzed for 3 hours against the same buffer but with reduced salt (500 mM NaCl) and applied to a Cytiva HisTrap FF crude 1 mL column on an ÄKTA Purifier 10 System equilibrated in the same buffer. The column was washed for 15 column volumes with the same buffer but containing 25 mM imidazole and protein subsequently eluted by increasing imidazole to 500 mM. The eluted protein sample was further purified using a Superdex75 16/60 gel filtration column (Cytiva) equilibrated in gel filtration buffer (10 mM HEPES-NaOH, pH 7.6, 300 mM NaCl, and 2 mM β-mercaptoethanol).

RsmI variants were generated using a whole plasmid PCR method (MEGAWHOP) using primers for first round PCR (to generate the “mega” primers) listed in *SI Appendix*, **Table S3**. RsmI variants were expressed as described above for the wild-type protein. A simplified purification strategy was used for wild-type and variant RsmI proteins for use in functional assays, using NEBExpress Ni Spin Column for affinity purification with minor modifications: three wash steps were done with increasing imidazole concentrations of 25, 50, and 100 mM before elution with 500 mM imidazole. Protein folding/ stability and prep-to-prep quality control was done using nano differential scanning fluorimetry on a NanoTemper Tycho NT.6.

Cryo-EM image processing–Following the workflow in CryoSPARC outlined in *SI Appendix***, Fig. S2,** movies were dose-weighed and corrected for motion drift using Patch Motion Correction with the output micrographs down sampled by a binning factor of 0.5. The contrast transfer function (CTF) was estimated using Patch CTF Estimation, and images with a CTF fit resolution > 5 Å were discarded (*SI Appendix*, **Fig. S2A**). Automatic blob picking selected 3,781,314 particles, which then underwent particle picking followed by extraction with a box size of 448 pixels, down-sampled to 128 pixels for initial particle curation, resulting in an initial set of 2,140,666 particles (*SI Appendix*, **Fig. S2B**). A series of 2D classification jobs to remove non-30S junk decreased the particle count to 1,380,845 and was followed by 3D particle sorting through iterative rounds of *ab initio* reconstruction and heterogenous refinement to further improve the dataset. Through this process, the resulting 938,684 30S particles were split into six reconstructions differing only in their occupancy of RsmI (*SI Appendix*, **Fig. S2B**). The reconstruction with highest RsmI occupancy (solid line box in *SI Appendix*, **Fig. S2B**), consisting of 356,021 particles (~38% of non-junk 30S particles), was retained for further refinement. Additionally, the reconstruction with the lowest occupancy of RsmI (288,883 particles; dashed line box in *SI Appendix*, **Fig. S2B**) was used as the starting point to generate a map for the free 30S-Δ*rsmI* after further processing (see below). The remaining 293,780 particles from the four reconstructions with intermediate RsmI occupancy were discarded (*SI Appendix*, **Fig. S4B**).

Particles with high RsmI occupancy were re-extracted at a box size of 448 pixels and underwent iterative rounds of Homogenous Refinement, Global CTF Refinement, Local CTF Refinement, and Reference Based Motion Correction to produce a final map of the complex at 2.12 Å (*SI Appendix*, **Fig.**

S2C). Further particle curation through iterative rounds of 3D Classification using a mask around the enzyme and accompanied by Heterogenous Refinement resulted in a decreased particle count of 264,656 particles, which formed a consensus 2.19 Å map after Homogenous Refinement. (*SI Appendix*, **Fig. S2D**). From this map, two separate strategies were employed. First, the particle density around RsmI and its 30S binding interface was subtracted and RsmI and its 30S contact surface locally refined using masked local refinement, leading to a 2.55 Å focused map (*SI Appendix*, **Fig. S2E**). For the second strategy, remnant 30S head-induced heterogeneity was removed and RsmI occupancy further improved through successive 3D classifications at low (16 Å) and high (6 Å) filter resolution, resulting in a final particle count of 74,553 particles. These particles underwent homogenous refinement followed by masked local refinement without particle subtraction, resulting in a 2.42 Å map of the entire complex (*SI Appendix*, **Fig. S2F**).

To generate a map for free 30S-Δ*rsmI* (*SI Appendix*, **Fig. S4B**), the 288,883 particles from the lowest-occupancy reconstruction after the initial 3D particle curation (dashed line box in *SI Appendix*, **Fig. S2B**) underwent further processing to remove as many particles with RsmI as possible. After additional iterative rounds of heterogenous refinement followed by successive 3D classification jobs filtered at 6 Å and 12 Å resolution, respectively, a collection of 58,000 particles remained with virtually no RsmI present. These particles were further refined following a similar strategy as described above to generate the final 2.91 Å final map for free 30S-Δ*rsmI*.

[^{3}H]-SAM methyltransferase assays to assess impact of 30S subunit activation and divalent metal ion identity on RsmI activity–Time course methylation assays to compare activated and non-activated 30S-Δ*rsmI* subunits as RsmI substrates were performed using the same [^{3}H]-SAM methyltransferase assay described in the main text *Materials and Methods*, except that aliquots quenched at 0, 2.5, 5, 10, 20, 40, and 60 minutes. Additional experiments in which 30S subunit substrate concentration was varied (25 to 400 nM) were conducted at 5 and 40-minute time points. All methylation data comparing activated and non-activated 30S-Δ*rsmI* were normalized to the highest non-activated 30S-Δ*rsmI* value.

Methylation assays with varying divalent ion (Mg^{2+}, Mn^{2+} or $Co(NH_3)_6^{3+}$) concentrations were conducted essentially identically other than variations in Buffer G to alter the final added magnesium acetate (0 to 10 mM), $MnCl_2$ (0 or 10 mM), or $Co(NH_3)_6^{3+}$ (0 to 1 mM). All assays also contained 0.27 mM magnesium acetate from the 30S subunit storage buffer. These data were normalized to the 10 mM Mg^{2+} condition for either RsmI or NpmA. All methylation assay data were plotted in GraphPad Prism 10.

RsmI conservation analysis–RsmI methyltransferase sequences were retrieved from UniProt using the InterPro identifier IPR018063. Sequence redundancy was removed by applying a 90% sequence identity cutoff (UniRef90) and clusters with fewer than 50 sequences were excluded. This process yielded a final set of 198 representative RsmI sequences, covering all major bacterial groups including Proteobacteria (Alpha-, Beta-, Gamma-, and others), Firmicutes, Actinobacteria, Cyanobacteria, and thermophilic bacteria. Multiple sequence alignment was performed in Geneious, and a neighbor-joining phylogenetic tree was generated to identify and isolate the Gammaproteobacterial RsmI clade. Residue propensities were calculated and sequence logos generated in Geneious software.

Isothermal titration calorimetry–SAM binding affinities for wild-type and E44A variant RsmI proteins were measured in triplicate using an Auto-iTC_{200}. Purified proteins were dialyzed exhaustively against gel filtration buffer lacking β-mercaptoethanol and the final dialysate was used to prepare the SAM solution (1 mM). Titrations were conducted at 25 ˚C and comprised 19 x 2 µl injections of SAM into the sample cell containing either wild-type RsmI or E44A (29-44 µM), with 120 s between injections to allow the power signal return to baseline. Raw titrations were processed (baseline and integration window adjustments, peak integration and subtraction of heats of dilution) and the resulting data integrated fit to a one site model via nonlinear regression using the modified Origin 7.0 software supplied with the instrument.